Research Paper
J. Astron. Space Sci. 35(1), 19-30 (2018)
https://doi.org/10.5140/JASS.2017.35.1.19

JASS Journal of Astronomy and Space Sciences

Magellanic Clouds Cepheids: Thorium Abundances

Yeuncheol Jeong[1], Alexander V. Yushchenko[2†], Vira F. Gopka[3], Volodymyr O. Yushchenko[3], Valery V. Kovtyukh[3], Svetlana V. Vasil'eva[3]

[1]Daeyang College, Sejong University, Seoul 05006, Korea
[2]Astrocamp Contents Research Institute, Goyang 10329, Korea
[3]Astronomical observatory, Odessa I.I. Mechnikov National University, Odessa 65014, Ukraine

The analysis of the high-resolution spectra of 31 Magellanic Clouds Cepheid variables enabled the identification of thorium lines. The abundances of thorium were found with spectrum synthesis method. The calculated thorium abundances exhibit correlations with the abundances of other chemical elements and atmospheric parameters of the program stars. These correlations are similar for both Clouds. The correlations of iron abundances of thorium, europium, neodymium, and yttrium relative to the pulsational periods are different in the Large Magellanic Cloud (LMC) and the Small Magellanic Cloud (SMC), namely the correlations are negative for LMC and positive or close to zero for SMC. One of the possible explanations can be the higher activity of nucleosynthesis in SMC with respect to LMC in the recent several hundred million years.

Keywords: abundances, variables: Cepheids, line: identification, nuclear reactions, nucleosynthesis, abundances, galaxies: Magellanic Clouds

1. INTRODUCTION

The investigation of stellar spectra allows us to find the chemical composition of the stellar atmosphere, which is a very thin layer at the surface of the star. The total mass of the atmosphere is negligible with respect to the mass of the star or to the mass of the interstellar environment in the Galaxy; nevertheless, the investigation of stellar atmospheres is the most reliable source of our knowledge on the chemical composition of the Universe. However, our information about stellar abundance patterns is not complete. Generally, the abundances of 20 to 30 chemical elements can be obtained by the investigation of the high-resolution spectrum of a bright star.

Examples for the best (by the number of investigated chemical elements) stellar abundance patterns are the prototype of rapidly oscillating Ap (roAp) stars, the Przybylski's star (Cowley et al. 2000; Shulyak et al. 2010) with 52 chemical elements heavier than hydrogen, the thorium-rich halo giant HD221170 (Yushchenko et al. 2005a; Ivans et al. 2006) with abundances of 46 elements and significant upper limits for an additional 5 elements, the HgMn star HD65949 (Cowley et al. 2010) with abundances of 41 and upper limits for 17 chemical elements, the hot metallic star Sirius (Landstreet 2011; Cowley et al. 2016) with 54 abundances and 25 upper limits, the mild barium star HD202109 (Yushchenko et al. 2004) with 51 abundances, the prototype of δ Sct-type stars, such as the δ Sct itself (Yushchenko et al. 2005b) with 49 abundances, and the δ Sct-type star ρ Pup (Yushchenko et al. 2015) with 56 abundances and 2 upper limits.

The abundances of 63 chemical elements are known in the solar photosphere (Grevesse et al. 2010), with thorium being the heaviest among them; the solar thorium abundance is logN(Th) = 0.03 ± 0.10 (Grevesse et al. 2015). The study of thorium clearly demonstrates the problems in the determination of chemical abundances of rare elements in stellar photospheres. The absorption lines of this element are very weak in the visible part of the spectra of the Sun and normal stars. Generally only the strongest line at wavelength λ4,019.129 Å has been used to find the thorium abundance in

Received 24 FEB 2018 **Revised** 8 MAR 2018 **Accepted** 8 MAR 2018
†**Corresponding Author**
Tel: +82-10-4093-5325, E-mail: avyushchenko@gmail.com
ORCID: https://orcid.org/0000-0002-9325-5840

the stars of our Galaxy.

Although this is the strongest line of thorium, it is heavily blended by lines of cobalt at λ4,019.126 Å, iron at λ4,019.044 Å, and by lines of other chemical elements. For this reason, the spectrum synthesis method has been used to investigate the thorium abundance in galactic stars using line λ4,019.126 Å only. One of the latest examples for this method can be found in a paper by Unterborn et al. (2015). To find fainter, but less blended thorium lines in the spectra of stars with normal chemical composition, it is necessary to use the ultraviolet spectra as it was shown by Yushchenko & Gopka (1994) for Procyon. The thorium abundance in this star was found by using four weak lines with wavelengths in the range of 3,262–3,468 Å.

In the case of stars with overabundance of neutron-captured elements, it is possible to use more thorium lines. A recent example is the study of the highly r-process-enhanced star RAVE J203843.2–002333 (Placco et al. 2017). Three thorium lines at wavelengths λ4,019.129 Å, λ4,086.521 Å, and λ4,094.747 Å were used in this study. The abundances of 39 chemical elements, including thorium and uranium were found. As indicated by the authors, the RAVE J203843.2–002333 is only the fourth star with measured uranium abundance among r-II stars of our Galaxy. r-II stars are the objects with r-process elemental-abundance ratios exceeding 10 times the solar values. These stars were defined by Beers & Christlieb (2005) as objects with [Eu/Fe] > 1.0 and [Ba/ Eu] < 0.0.

Yushchenko et al. (2005a) identified seven thorium lines in the spectrum of the thorium-rich halo star HD221170. One of these lines, specifically line λ5,989.045 Å was used by Gopka et al. (2005) and by Aoki et al. (2007) to find the thorium abundances in two red supergiants of the Small Magellanic Cloud (SMC) and in the red giant star of the Ursa Minor dwarf galaxy from the observations in red spectral region. These papers were the first to determine the thorium abundance for extragalactic objects. Later Gopka et al. (2007, 2013) identified several thorium lines in the spectra of red supergiants of the Magellanic Clouds, specifically lines λ5,989.045 Å, λ6,044.433 Å, λ6,112.837 Å, and λ6,619.944 Å. Yushchenko et al. (2017a, b) used the first and the first three of these lines and line λ6,693.037 Å to find the abundance of thorium in the atmospheres of RM_1-390 and PMMR 23, which are red supergiants in the Large and Small Magellanic Clouds, respectively.

The studies of thorium, cited above, show that the abundance of thorium can be obtained from different lines of this element, located in different spectral regions. The identification of these lines in the observed stellar spectra needs careful comparison with the synthetic spectra, calculated with different abundances of thorium and other chemical elements. This is the only way to investigate the abundances of any chemical element with low abundances and not numerous lines in the stellar spectra.

The thorium abundance allowed to find the ages of stars using the abundance ratios of thorium and other chemical elements and the assumption of the r-process universality, that is, the equal ratios of chemical elements production in different supernova events. Yushchenko et al. (2005a) showed that it results in unreliable age values for several thorium-rich stars. Later, Ren et al. (2012) found a wide scattering of thorium abundances in different stars of up to 4 dex, and highlighted the problem of using the Th/Eu ratio to derive stellar ages.

The universality of supernova explosions is also disputed by other observational facts. Even a decade earlier supernovas were accepted as the most probable end of the evolutionary history of massive stars. The results of the photometric survey of 106 red supergiants in the nearby galaxies (Kochanek et al. 2008) enabled the discovery of four supernova events and the disappearance of one supergiant (Gerke et al. 2015; Adams et al. 2017). By taking the observational selection into account, specifically the more reliable detection of an outburst compared to that of a disappearance, it is possible to conclude that a gravitational collapse without a supernova event is the most common scenario for the evolution of stars with masses over 18 solar masses (Smartt 2015).

The observational results dispute the existence of a compact body in the remnant of SN1987A at the luminosity level near a few tens of solar luminosities (McCray & Fransson 2016). The results of observations and numerical simulations of asymmetric Supernova explosions should also be mentioned. Popov et al. (2014) found that different chemical elements can be ejected in different directions. Björnsson & Keshavarzi (2017) analyzed the observations of supernovas in the radio wavelength region and indicated the high probability of the inhomogeneous structure of the sources. It seems reasonable to conclude that the final stages of stellar evolution can be very different, the universality assumption for supernova explosions cannot be accepted, and determining stellar ages using thorium abundances needs to be avoided. A recent example of age determination using thorium and uranium abundances can be found in the study by Placco et al. (2017) cited above. Fig. 6 in the publication by Placco et al. (2017) shows the scattering of age determination values for different pairs of chemical elements from 25 billion years to negative values, which is the reason the authors accept only the values which give results close to 13 billion years.

Preferably, we avoid the use of thorium for stellar age determination. Thorium abundances are very important for the investigation of the r-process productivity in supernova

events. In this study, we analyze the lines of thorium in supergiant stars, specifically in the atmospheres of 31 Cepheid variables located in the Large and Small Magellanic Clouds, and present the thorium abundances and their correlations with stellar atmosphere parameters, pulsational periods, and abundances of other chemical elements.

The spectra were obtained in the red spectral region, with the strongest thorium line λ4,019.044 Å outside the observed region, which is the reason for using four fainter lines with longer wavelengths.

2. OBSERVATIONS, ATMOSPHERE PARAMETERS, AND LINE IDENTIFICATIONS

The used spectra of the 31 Cepheid variables in the Large and Small Magellanic Clouds were observed from October to December 2000, at the Very Large Telescope (VLT) array with the ultraviolet and visual echelle spectrograph (UVES) in the frames of observational run 66.D-0571(A) with the metallicity effect on the Cepheid period-luminosity relation. The principal investigator was M. Groenewegen. The reduced spectra were taken from the public European Southern Observatory (ESO) archive. The wavelength region was 4,760–6,820 Å, the spectral resolving power was close or exceeding R = 30,000, and the signal-to-noise ratio was S/N = 30–70. The used spectra were obtained by Romaniello et al. (2008) and Chekhonadskikh (2012) found the effective temperatures, surface gravities, microturbulent velocities, and determined the abundances of 20 chemical elements from carbon to europium with the model atmospheres method. The used effective temperatures of the stars were in the range of 4,662–6,300 K, the surface gravities were in the range of log$g$ = 0.2–1.9. We calculated the synthetic spectra of these stars in the observed wavelength region, by using the program SYNTHE by Kurucz (1993). The continuum placement was made by the URAN software (Yushchenko 1997). The details of the synthetic spectra calculations and reduction procedure are similar to those described by Yushchenko et al. (2015), Kang et al. (2013), and Jeong et al. (2017).

The comparison of the observed and synthetic spectra allows the estimation of line broadening in the observed spectra. It is assumed that the line broadening in the observed spectra is the result of the instrumental profile of the spectrograph and the macroturbulent velocities in the stellar atmospheres. The Gaussian model of macroturbulence was applied (Gray 1976), and the clean lines of iron were used to find the values of macroturbulent velocities for all stars.

The identification of thorium lines in the observed spectra was made by using the URAN software (Yushchenko 1997), based on the comparison of the observed and synthetic spectra. The synthetic spectra were calculated for all program stars with atmosphere models and abundances published by Chekhonadskikh (2012). Those abundances of elements that were not found by Chekhonadskikh (2012) were assumed to be similar to the abundances of elements with close atomic numbers or estimated. After several iterations the appropriate coincidence of observations and calculations was achieved for the whole wavelength interval of the used spectral observations. The inspection of all thorium lines in the investigated wavelength region allows the selection of only four lines to determine the abundance. The rest of the thorium lines appeared to be very weak, or heavily blended, or located near the edges of the echelle orders.

Table 1. Lines used for thorium

l (Å)	E_{low} (eV)	loggf
5,055.347	0.189	-1.923
5,639.746	0.189	-1.605
5,989.045	0.189	-1.414
6,112.837	0.231	-1.832

These four lines are listed in Table 1. The columns of the table are wavelengths, low-level energies, and oscillator strengths. The values of the oscillator strengths were taken from Nilsson et al. (2002). The observed profiles of these lines in the spectrum of one of program stars, HV 5497 are shown in Fig. 1. Lines λ5,055.347 Å and λ6,112.837 Å were faint and detected only in a few stars. Thorium line λ6,112.837 Å is strongly blended by the Si I λ6,112.928 Å line. Line λ5,639.746 Å was identified only in the cool stars of our sample, and only line λ5,989.045 Å was strong enough to be identified in all stars. We tried to identify all mentioned four thorium lines in all program stars, as well as other lines of this element, but the measurable absorptions were found only for lines, listed in Table 1.

3. THORIUM ABUNDANCES

The thorium abundances in the program stars were found by the spectrum synthesis method. The fit of the observed spectrum by the calculated spectrum was made in semiautomatic mode using the SYNTHE (Kurucz 1993) and URAN (Yushchenko 1997) codes. The calculations for all stars were made with four atmosphere models. The parameters of the first model for each star were selected in accordance with the paper by Chekhonadskikh (2012). The parameters of the three additional models were slightly altered by an effective increase of 100 K in temperature, an increase of 0.5 dex in gravity, and an increase of 1.0 km s^{-1} in microturbulence velocity. The models with the required parameters were interpolated from

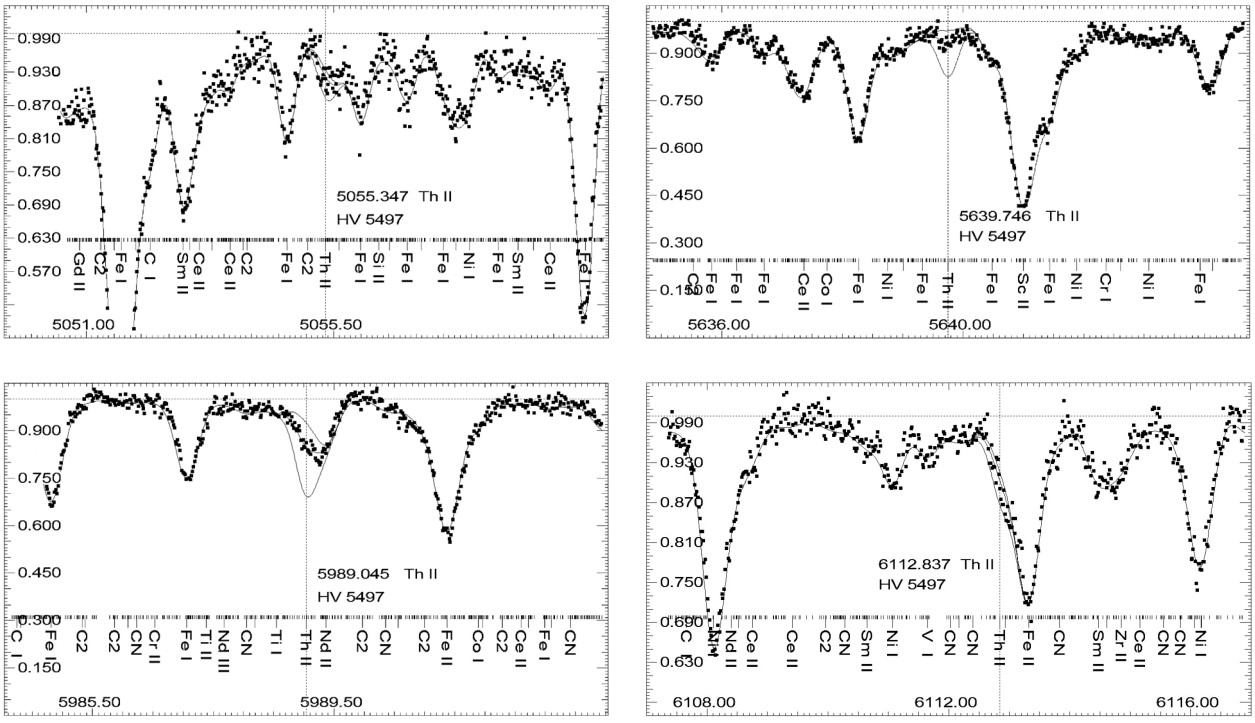

Fig. 1. Spectrum of HV 5497 in the vicinities of four thorium lines λ5,055.347 Å, λ5,639.746 Å, λ5,989.045 Å, and λ6,112.837 Å. The position of these lines is marked by a dotted vertical line. The axes represent the wavelength in angstroms and the relative flux. The filled squares denote the observed spectrum. The fit of the observed spectrum by the synthetic spectrum is shown by three thin lines. Three lines were calculated with the best thorium abundance and the abundances deviated by ±0.5 dex from the best value. The positions of the spectral lines, considered in the calculations, are marked in the bottom part of the figure by short and long dashes (faint and strong lines). The identifications are shown for some of the strongest lines.

the grid of the atmosphere models for Large Magellanic Cloud (LMC) stars by Kurucz (1993) and from the grid of the models for SMC stars by Castelli & Kurucz (2003). More details about the calculation procedure can be found in recent papers by Yushchenko et al. (2015, 2017b) and Kim et al. (2007). Table 2 lists the results of the abundance calculations for all lines used.

The first three columns of Table 2 are the star name, wavelength of the line used, and thorium abundance. The fourth column is the relative part of the thorium line in the total line absorption coefficient at the wavelength of the investigated line. For clean lines this value is close to 1.00, for heavily blended lines it becomes close to zero. The fifth column is the depth of the synthetic spectrum at the wavelength of the thorium line. The values of the fourth and fifth columns were calculated using the synthetic spectra, unsmoothed by the macroturbulence and instrumental profiles.

Columns six to eight present corrections to the values of thorium abundances presented in the third column for the case of calculations with altered atmosphere models. The ninth column is the value of the synthetic spectrum at the wavelength of the thorium line, calculated with the best thorium abundance and convolved with the observational and macroturbulence profiles, which is expected to be similar to the value of the observed spectrum at this wavelength. The last two columns are similar values to the synthetic spectrum, calculated with thorium abundance decreased and increased by 0.5 dex, respectively.

Fig. 1 shows a fit of observations by the synthetic spectra for thorium lines in the spectrum of HV 5497. Three synthetic spectra were calculated with the best thorium abundances, and the abundances decreased and increased with respect to the best value by 0.5 dex. These spectra coincide for all wavelengths except those in the vicinities of thorium lines. The deviations of the synthetic spectra illustrate the accuracy of the determined abundance. As it was discussed in the previous section the abundances derived using lines λ5,055.347 Å and λ6,112.837 Å are less reliable than the values calculated with lines λ5,639.746 Å and λ5,989.045 Å.

Table 3 contains the main result of this study; the mean values of thorium abundances in the Magellanic Clouds Cepheid variables. The first column is the designation of the program star, the second to fifth columns are taken from the paper by Chekhonadskikh (2012) and show the parameters of the atmosphere model and iron abundance. Column six is the number of thorium lines identified in the observed spectrum. The last four columns are the mean thorium

Table 2. Thorium lines in the spectra of Magellanic Clouds Cepheid variables

Star	Wavelength (Å)	logN	%	R	ΔlogN			R_{best}	ΔR_{best}	
					T_{eff}+ 100 K	log*g*+ 0.5	V_{turb}+ 1 km s^{-1}		logN -0.5	logN 0.5
1	2	3	4	5	6	7	8	9	10	11
LMC stars										
HV 877	5,055.347	0.476	0.39	0.057	0.169	0.021	0.011	0.109	-0.018	0.053
	5,639.746	0.419	0.82	0.099	0.054	0.127	0.013	0.089	-0.035	0.093
	5,989.045	0.548	0.88	0.186	0.032	0.185	0.011	0.146	-0.065	0.145
HV 879	5,989.045	0.774	0.97	0.117	0.059	0.145	0.014	0.075	-0.039	0.099
HV 971	5,989.045	0.730	0.97	0.108	0.161	-0.131	-0.055	0.069	-0.025	0.066
HV 997	5,989.045	0.659	0.95	0.070	0.097	0.159	0.157	0.056	-0.018	0.049
HV 1013	5,989.045	-0.053	0.73	0.124	0.134	0.046	0.011	0.120	-0.028	0.071
	6,112.837	-0.066	0.31	0.044	0.137	0.165	0.173	0.097	-0.009	0.026
HV 1023	5,989.045	0.877	0.98	0.117	-0.052	0.083	0.013	0.053	-0.025	0.065
HV 2260	5,989.045	0.606	0.95	0.059	0.164	-0.003	-0.003	0.042	-0.012	0.033
HV 2294	5,639.746	0.708	0.98	0.171	-0.042	0.087	0.063	0.083	-0.047	0.110
	5,989.045	0.714	0.97	0.245	0.068	0.125	0.130	0.147	-0.077	0.152
	6,112.837	0.795	0.80	0.117	0.110	0.142	0.075	0.087	-0.035	0.088
HV 2337	5,989.045	0.879	0.98	0.183	0.040	0.130	-0.029	0.071	-0.040	0.090
HV 2352	5,989.045	0.407	0.77	0.018	-0.059	0.172	0.006	0.017	-0.005	0.017
HV 2369	5,639.746	0.137	0.89	0.152	-0.017	-0.068	-0.049	0.103	-0.029	0.072
	5,989.045	0.073	0.86	0.193	-0.012	0.042	-0.058	0.117	-0.037	0.083
HV 2405	5,989.045	0.576	0.75	0.041	-0.083	-0.004	0.096	0.042	-0.012	0.035
HV 2580	5,989.045	0.575	0.97	0.157	-0.140	-0.100	-0.031	0.073	-0.033	0.078
	6,112.837	0.483	0.53	0.049	-0.012	0.072	0.181	0.056	-0.009	0.027
HV 2733	5,989.045	0.562	0.95	0.084	0.080	0.142	0.062	0.043	-0.020	0.054
HV 2793	5,989.045	0.532	0.97	0.158	0.033	0.194	0.046	0.077	-0.032	0.077
HV 2827	5,055.347	0.207	0.37	0.069	0.140	0.078	0.132	0.117	-0.014	0.040
	5,639.746	0.440	0.95	0.211	-0.036	0.100	-0.044	0.123	-0.062	0.134
	5,989.045	0.349	0.90	0.251	0.013	0.110	0.060	0.182	-0.069	0.138
	6,112.837	0.261	0.47	0.084	0.139	0.040	0.037	0.125	-0.021	0.057
HV 2836	5,639.746	0.143	0.93	0.041	0.055	0.110	0.054	0.019	-0.010	0.031
	5,989.045	0.237	0.94	0.075	0.106	0.165	0.010	0.047	-0.020	0.057
HV 2864	5,989.045	0.769	0.96	0.114	0.074	0.163	0.021	0.047	-0.021	0.055
HV 5497	5,055.347	0.341	0.49	0.046	0.077	0.012	-0.041	0.066	-0.013	0.040
	5,639.746	0.386	0.95	0.099	0.084	0.132	-0.003	0.056	-0.032	0.085
	5,989.045	0.629	0.97	0.232	0.053	0.142	-0.013	0.155	-0.074	0.150
	6,112.837	0.394	0.32	0.056	0.049	-0.027	0.063	0.129	-0.014	0.041
HV 12452	5,989.045	0.659	0.97	0.123	0.036	0.120	-0.124	0.066	-0.030	0.075
HV 12700	5,989.045	0.769	0.97	0.178	0.072	0.171	0.019	0.087	-0.048	0.109
SMC stars										
HV 817	5,989.045	0.422	0.95	0.052	0.057	0.172	0.008	0.033	-0.014	0.042
HV 824	5,639.746	0.412	0.99	0.100	0.064	0.145	0.007	0.043	-0.026	0.070
	5,989.045	0.590	0.99	0.206	0.057	0.153	0.000	0.101	-0.055	0.117
	6,112.837	0.631	0.97	0.088	0.065	0.165	-0.008	0.045	-0.023	0.063
HV 829	5,639.746	0.575	0.98	0.105	0.056	0.145	0.013	0.059	-0.037	0.098
	5,989.045	0.360	0.96	0.099	0.056	0.150	-0.002	0.077	-0.035	0.091
	6,112.837	0.659	0.93	0.069	0.078	0.187	0.010	0.051	-0.024	0.068
HV 834	5,639.746	0.621	0.95	0.034	0.055	0.130	0.023	0.018	-0.011	0.033
	5,989.045	0.975	0.97	0.109	0.071	0.133	0.016	0.060	-0.035	0.090
HV 837	5,989.045	0.477	0.99	0.172	0.050	0.167	0.015	0.087	-0.046	0.106
	6,112.837	0.658	0.97	0.097	0.066	0.130	-0.008	0.046	-0.026	0.069
HV 847	5,055.347	-0.208	0.27	0.038	0.262	0.170	0.132	0.094	-0.008	0.025
	5,639.746	0.278	0.97	0.204	0.044	0.161	0.005	0.109	-0.063	0.138
	5,989.045	-0.087	0.93	0.145	0.059	0.163	0.005	0.088	-0.044	0.107
HV 1954	5,989.045	0.144	0.62	0.022	0.110	0.134	0.165	0.029	-0.006	0.020
HV 2064	5,989.045	0.302	0.92	0.041	0.074	0.064	-0.011	0.032	-0.012	0.037
HV 2195	5,989.045	0.539	0.92	0.030	0.059	0.128	0.012	0.020	-0.011	0.034
HV 11211	5,989.045	-0.459	0.83	0.042	0.147	0.025	0.080	0.025	-0.011	0.032

Table 3. Atmospheric parameters used and the derived mean values of the thorium abundances

Star	T_{eff} (K)	log*g*	V_{turb} (km s^{-1})	[Fe-H]	n	logN	logN		
							T_{eff}+ 100 K	log*g*+ 0.5	V_{turb}+ 1 km s^{-1}
1	2	3	4	5	6	7	8	9	10
LMC stars									
HV 877	4,831	1.0	6.0	-0.25	3	0.48(05)	0.57(07)	0.59(10)	0.49(05)
HV 879	5,809	1.2	5.3	-0.11	1	0.77	0.83	0.92	0.79
HV 971	5,943	1.9	4.0	-0.36	1	0.73	0.89	0.60	0.67
HV 997	5,782	1.5	6.0	-0.28	1	0.66	0.76	0.82	0.82
HV 1013	4,662	0.3	5.3	-0.40	2	-0.06(00)	0.08(00)	0.05(05)	0.03(07)
HV 1023	5,909	1.5	4.5	-0.18	1	0.88	0.82	0.96	0.89
HV 2260	5,898	1.8	4.0	-0.06	1	0.61	0.77	0.60	0.60
HV 2294	5,232	0.9	5.0	-0.16	3	0.74(03)	0.78(09)	0.86(05)	0.83(04)
HV 2337	5,489	1.5	4.5	-0.12	1	0.88	0.92	1.01	0.85
HV 2352	6,300	1.8	5.5	-0.26	1	0.41	0.35	0.58	0.41
HV 2369	4,794	0.2	4.0	-0.11	2	0.11(03)	0.09(02)	0.09(02)	0.05(03)
HV 2405	5,985	1.8	5.0	-0.24	1	0.58	0.49	0.57	0.67
HV 2580	5,461	1.2	3.5	-0.06	2	0.53(04)	0.45(01)	0.51(03)	0.60(06)
HV 2733	5,473	1.6	5.0	-0.25	1	0.56	0.64	0.70	0.62
HV 2793	5,505	1.0	3.5	-0.07	1	0.53	0.56	0.73	0.58
HV 2827	4,892	0.3	4.7	-0.20	4	0.31(08)	0.38(02)	0.40(10)	0.36(04)
HV 2836	5,471	1.1	4.0	-0.13	2	0.19(04)	0.27(07)	0.33(07)	0.22(02)
HV 2864	5,799	1.6	3.7	-0.17	1	0.77	0.84	0.93	0.79
HV 5497	5,206	0.6	6.1	-0.29	4	0.44(11)	0.50(10)	0.50(16)	0.44(11)
HV 12452	5,548	1.5	4.0	-0.16	1	0.66	0.69	0.78	0.53
HV 12700	5,451	1.4	4.1	-0.22	1	0.77	0.84	0.94	0.79
SMC stars									
HV 817	5,940	1.4	4.7	-0.61	1	0.42	0.48	0.59	0.43
HV 824	5,333	1.1	4.5	-0.54	3	0.54(09)	0.61(09)	0.70(10)	0.54(08)
HV 829	5,350	1.0	7.0	-0.62	3	0.53(12)	0.59(13)	0.69(13)	0.54(13)
HV 834	6,016	1.6	6.0	-0.38	2	0.80(17)	0.86(18)	0.93(17)	0.82(17)
HV 837	5,355	1.0	4.6	-0.55	2	0.57(09)	0.63(09)	0.72(07)	0.57(07)
HV 847	4,817	0.4	4.5	-0.66	3	-0.01(20)	0.12(14)	0.16(20)	0.04(17)
HV 1954	5,974	1.6	5.2	-0.61	1	0.14	0.25	0.28	0.31
HV 2064	5,832	1.5	5.3	-0.39	1	0.30	0.38	0.37	0.29
HV 2195	6,211	1.6	6.8	-0.47	1	0.54	0.60	0.67	0.55
HV 11211	5,067	0.8	4.0	-0.58	1	-0.46	-0.31	-0.43	-0.38

abundances in the atmosphere of this star. The first of them is calculated with atmosphere parameters presented in the paper by Chekhonadskikh (2012), the next three columns are atmosphere models slightly altered by an effective increase of 100 K in temperature, an increase of 0.5 dex in gravity, and an increase of 1.0 km s^{-1} in microturbulence velocity, respectively. The last figures of errors are shown in brackets. The errors were calculated as the square roots of the sum of squares of deviations of the individual values of abundances from the mean value divided by the number of lines used.

To compare the thorium abundances in the atmospheres of Magellanic Cloud Cepheid variables with those in our Galaxy we tried to find thorium lines in the high quality spectrum of the galactic Cepheid V473 Lyr (Andrievsky et al. 1998), but no measurable lines were found. The strongest thorium line λ5,055.347 Å is heavily blended by lines of other chemical elements, while the other thorium lines are faint and do not allow the calculation of the thorium abundance.

4. DISCUSSION

The thorium lines were not identified and the thorium abundances were not measured in the atmospheres of any extragalactic objects, including the atmospheres of Magellanic Clouds Cepheid variables, except for certain cases cited in the Introduction section. Therefore finding the observed correlations of thorium abundances with different parameters of Cepheid variables is of interest to us.

Fig. 2 shows the absolute values of thorium abundances in the program stars as a function of effective temperatures, surface gravities, metallicities, and europium abundances. Henceforth, the abundances of all chemical elements (except thorium) used are in accordance with the paper

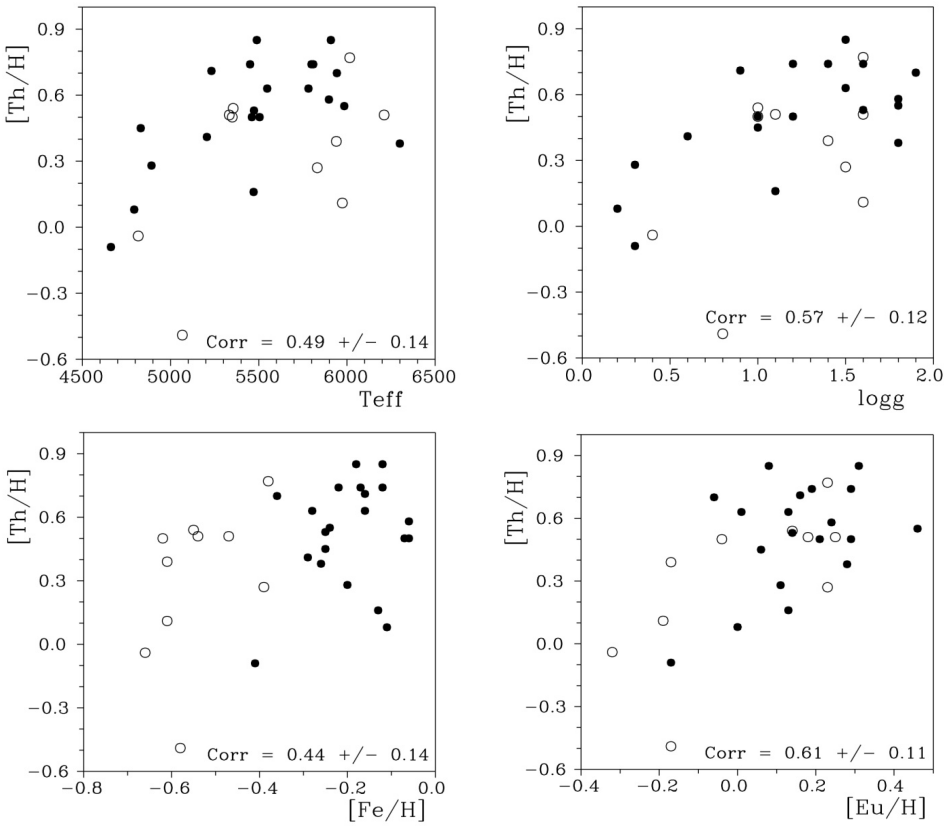

Fig. 2. Plots of thorium abundances in the program stars as a function of effective temperature, surface gravity, iron and europium abundance. Filled and open circles represents the LMC and SMC stars, respectively. The correlation coefficients with errors are shown in the low right corners.

by Cheknonadskikh (2012). The correlation coefficients of thorium abundance as a function of the parameters mentioned above are positive. The thorium abundances increase with the increase of the effective temperatures, surface gravities, metallicities, and europium abundances. The dependencies are similar in both Clouds.

It is generally accepted that Cepheid variables are young massive stars. It is also accepted that thorium is the result of r-process nucleosynthesis. The standard theory of stellar evolution rejects the possibility of the r-process in usual stars. The exceptions are supernova explosions, the accretion events in relativistic objects such as white dwarfs and neutron stars, and similar catastrophic events. The possible sites of occurrence of the r-process are still under discussion; nevertheless, supernova explosions should be one of the most probable site.

Thus, Fig. 2 should reflect the change of abundances of r-process elements in the interstellar medium during the time between the creation of the oldest and the youngest objects of our sample. The older the variables are, the shorter pulsational period is. In accordance with Anderson et al. (2016) the ages of all our program stars are less than three hundred million years. The older Cepheid variables are expected to have higher temperatures and higher surface gravities. Thus, the upper panels of Fig. 2 show the decrease of thorium abundances in the interstellar medium between the creation of the oldest and the youngest stars of our sample.

The lower left panel of Fig. 2 shows the thorium abundance with respect to metallicity. The metallicity is expected to increase with time; an example is the difference in metallicity between the disk and the halo stars of our Galaxy. It is generally accepted that halo stars are older than disk stars.

Therefore, the increase of metallicity corresponds to younger stars and the discussed panel suggests that the thorium abundance increases in the interstellar medium with time. This result is in disagreement with the trend discussed and shown in the upper panels of Fig. 2. LMC and SMC stars are located in different areas of this panel, but the trends are similar for both Clouds.

The lower right panel of Fig. 2 and the four panels of Fig. 3 show the correlation of thorium abundances in our stars with the abundances of Eu, Y, Nd, Sc, and Ni. The abundances

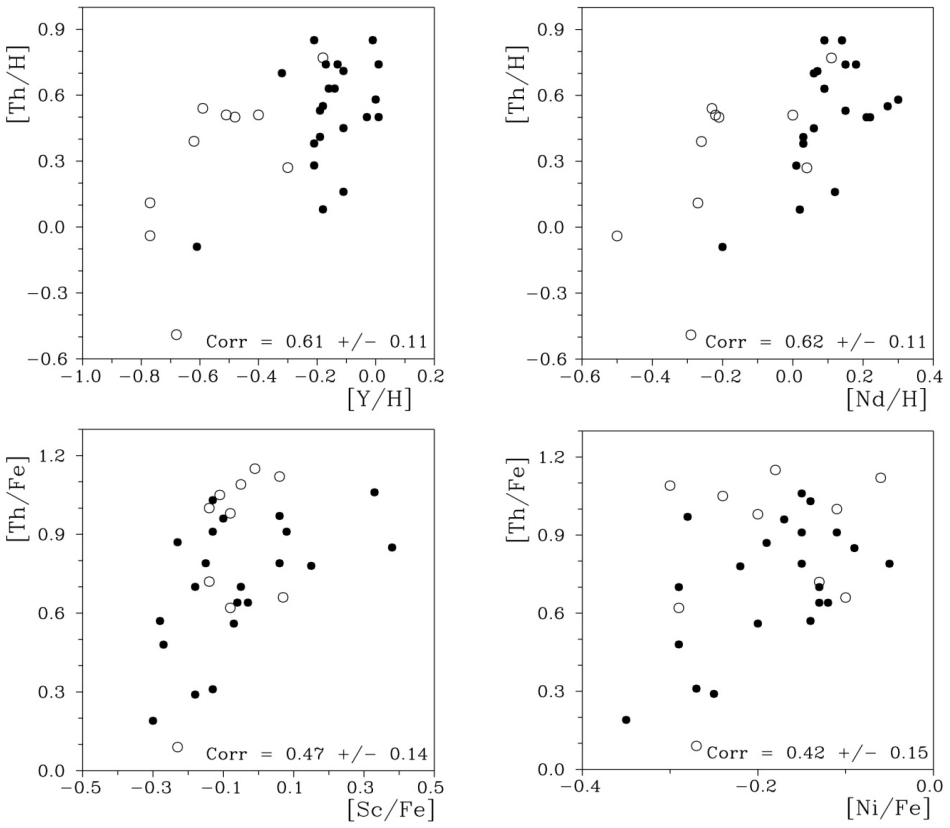

Fig. 3. Plots of thorium abundances in the program stars as a function of Y, Nd, Sc, and Ni abundance. Filled and open circles represents the LMC and SMC stars, respectively. The upper panels represent the abundances with respect to hydrogen, while the lower – with respect to iron. The correlation coefficients with errors are shown in the low right corners.

of thorium increase with the increase of the abundances of these elements. These trends can be seen for both Clouds. It should be noted that Eu and Nd is expected to be produced in a neutron capture r-process simultaneously with thorium, thus, the positive correlations shown in Figs. 2 and 3 for these elements seem straightforward.

Currently we are not able to explain the correlations of thorium abundances with the abundances of Y, Sc, and Ni. As it was indicated before, thorium abundances were not measured in extragalactic objects previously.

Cepheid variables were discovered as objects with periodic changes in their luminosity. The periods of light variations can be regarded as the main feature of Cepheids, which are known with higher accuracy than any other characteristics of these stars. Thus, it seems reasonable to compare the abundances of chemical elements with the periods. Fig. 4 shows the relative abundances of Th, Eu, Nd, and Y as a function of pulsational period. The values of the periods for the program stars were collected from different sources by Romaniello et al. (2008) and Chekhonadskikh (2012), and references can be found in these papers.

The longer periods are expected to correspond to the younger stars. Fig. 4 shows the evolution of relative abundances in the interstellar environment with time. It should be noted that the trends for LMC and SMC objects are different, and the correlations coefficients confirm these discrepancies.

The abundances of Th, Eu, Nd, and Y in the atmosphere of LMC stars relative to iron show a negative or near-zero correlation with the period. The same correlations for SMC objects are positive.

The possible explanation for the case of the LMC is that the production of these elements in supernova explosions and other similar events is relatively low and does not follow the rate of light element synthesis.

For the case of the SMC it can be assumed that the rate of the r-process elements synthesis to higher than that of the lighter elements. Therefore, the relative number of supernova explosions and similar catastrophic events where the r-process can take place is higher in the SMC compared to those of the LMC, and also compared to our Galaxy. It should be noted that the SMC is known as a galaxy with higher number of young stars (compared to the Galaxy).

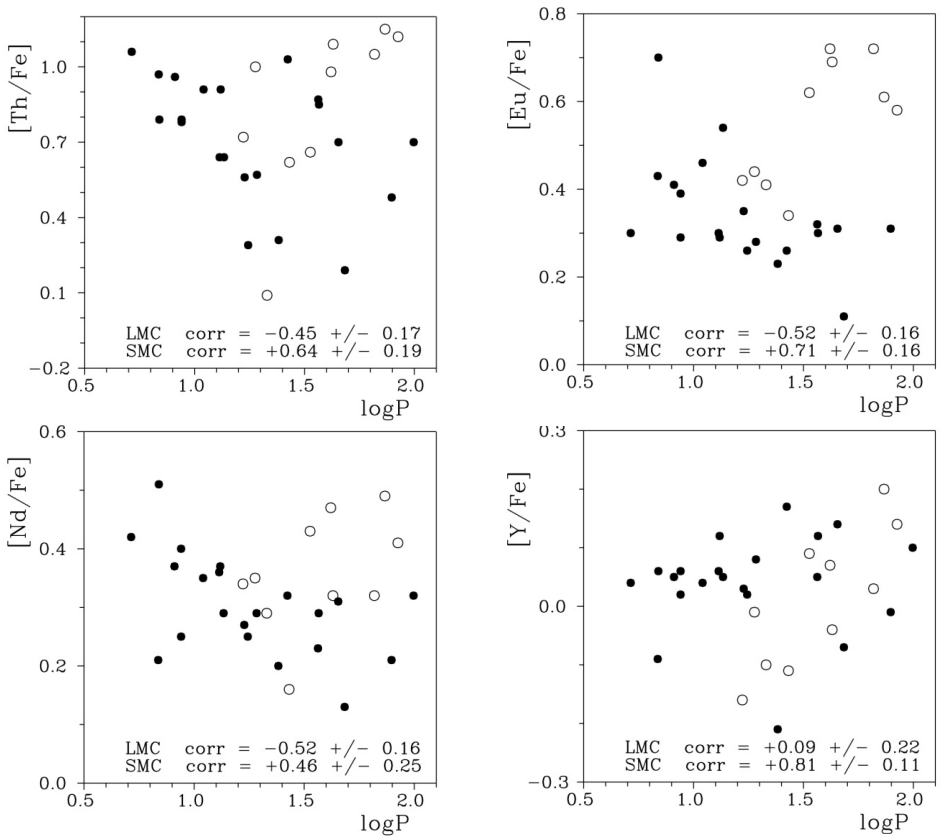

Fig. 4. Plots of element to iron abundance ratios in the program stars as a function of pulsational period. Filled and open circles represent the LMC and SMC stars, respectively. The correlation coefficients with errors are shown in the lower part of the panels for LMC and SMC objects.

As an example, it is possible to compare the number of Be/X-ray binary systems in SMC and our Galaxy. The number of these systems in the LMC is similar to that in our Galaxy (Coe et al. 2011), but the Galaxy is much more massive than SMC, that is why it supports the conclusion of higher rate of r-procees nucleosynthesis in SMC.

5. CONCLUSION

In this paper, the first detection of thorium in one type of extragalactic objects is presented. The comparison of high-resolution spectral observations of thirty-one Cepheid variables in the Large and Small Magellanic Clouds with the synthetic spectra enabled the identification of thorium absorption lines. The oscillator strengths of these lines were obtained from the work by Nilsson et al. (2002). It is worth to mention that the identified thorium lines are very faint in the solar spectrum. That is why the direct comparison with solar abundances is impossible and the result strongly depends on the choice of oscillator strengths. The abundances of thorium were calculated by the spectrum synthesis method.

It is necessary to point the importance of thorium lines identification in the visual part of the spectrum. Many bright extragalactic objects can be observed in this wavelength range. The used method of line identification, namely the comparison of observed and calculated spectra in wide wavelength range allows finding of absorption lines, which were not investigated earlier.

The analysis of the derived thorium abundances, abundances of other chemical elements, atmosphere parameters, and pulsational periods allows to find several interesting correlations:

1) Thorium abundances increase with the increase of the effective temperature, surface gravity, and metallicity of the star
2) Thorium abundances increase with the increase of the abundances of Eu, Nd, Y, Sc, and Ni.
3) Thorium abundances changes with the pulsational period of the star. The correlation is negative for the LMC and positive for the SMC. Similar correlations are found for Eu, Nd, and Y.

It is necessary to point that the number of investigated objects can be not sufficient, and the analysis of additional stars can change these correlations. It will be interesting to investigate more r-, s-process elements abundances in these stars. The high europium and thorium abundances can be the sign of possible higher abundances of other neutron capture elements in the atmospheres of Magellanic Clouds Cepheid variables. Several of these dependencies are still not fully understood, and require a more detailed analysis of the existing spectra and new observations of Cepheid variables in the Magellanic Clouds, as well as in other Local Group galaxies. Astronomy is based on observations, new observations often show unexpected results, and theory generally follows experimental observations.

ACKNOWLEDGMENTS

One of the authors (VYu) was supported by the Swiss National Science Foundation (SCOPES project No. IZ73Z0152485).

REFERENCES

Adams SM, Kochanek CS, Gerke JR, Stanek KZ, Dai X, The search for failed supernovae with the Large Binocular Telescope: confirmation of a disappearing star, Mon. Not. R. Astron. Soc. 468, 4968-4981 (2017). https://doi.org/10.1093/mnras/stx816

Anderson RI, Saio H, Ekström S, Georgy C, Meynet G, On the effect of rotation on populations of classical Cepheids. II. Pulsation analysis for metallicities 0.014, 0.006, and 0.002, Astron. Astrophys. 51, A8 (2016). https://doi.org/10.1051/0004-6361/201528031

Andrievsky SM, Kovtyukh VV, Bersier D, Luck RE, Gopka VP, et al., The unique galactic Cepheid V473 Lyrae revisited, Astron. Astrophys. 329, 599-605 (1998).

Aoki W, Honda S, Sadakane K, Arimoto N, First determination of the actinide thorium abundance for a red giant of the Ursa minor dwarf galaxy, Publ. Astron. Soc. Jpn. 59, L15-L19 (2007). https://doi.org/10.1093/pasj/59.3.L15

Beers TC, Christlieb N, The discovery and analysis of very metal-poor stars in the Galaxy, Annu. Rev. Astron. Astrophys. 43, 531-580 (2005). https://doi.org/10.1146/annurev.astro.42.053102.134057

Björnsson C-I, Keshavarzi ST, Inhomogeneities and the modeling of radio supernovae, Astrophys. J. 841, 12 (2017). https://doi.org/10.3847/1538-4357/aa6cad

Castelli F, Kurucz RL, New Grids of ATLAS9 Model Atmospheres, Proceedings of the IAU Symposia 210: Modelling of Stellar Atmospheres, Uppsala University, Uppsala, Sweden, 17-21 June 2002.

Chekhonadskikh FA, Abundances and absolute stellar magnitudes for F and G supergiants of Magellanic Clouds, Kinemat. Phys. Celest. Bodies 28, 128-136 (2012). https://doi.org/10.3103/S0884591312030026

Coe MJ, Haberl F, Sturm R, Pietsch W, Townsend LJ, et al., The XMM-Newton survey of the Small Magellanic Cloud: XMMU J005011.2-730026 = SXP 214, a Be/X-ray binary pulsar, Mon. Not. R. Astron. Soc. 414, 3281-3287 (2011). https://doi.org/10.1111/j.1365-2966.2011.18626.x

Cowley CR, Ryabchikova T, Kupka F, Bord DJ, Mathys G, et al., Abundances in Przybylski's star, Mon. Not. R. Astron. Soc. 317, 299-309 (2000). https://doi.org/10.1046/j.1365-8711.2000.03578.x

Cowley CR, Hubrig S, Palmeri P, Quinet P, Biémont É, et al., HD 65949: Rosetta stone or red herring, Mon. Not. R. Astron. Soc. 405, 1271-1284 (2010). https://doi.org/10.1111/j.1365-2966.2010.16529.x

Cowley CR, Ayres TR, Castelli F, Gulliver AF, Monier R, et al., A study of the elements copper through uranium in Sirius A: contributions from STIS and ground-based spectra, Astrophys. J. 826, 158 (2016). https://doi.org/10.3847/0004-637X/826/2/158

Gerke JR, Kochanek CS, Stanek KZ, The search for failed supernovae with the Large Binocular Telescope: first candidates, Mon. Not. R. Astron. Soc. 450, 3289-3305 (2015). https://doi.org/10.1093/mnras/stv776

Gopka V, Yushchenko A, Andrievsky S, Goriely S, Vasiléva S, et al., The abundances of chemical elements in the atmospheres of K-supergiants in the Small Magellanic Cloud and Arcturus, Proceedings of the IAU Symposia 228: From Lithium to Uranium: Elemental Tracers of Early Cosmic Evolution, Paris, France, 23-27 May 2005.

Gopka VF, Vasil'eva SV, Yushchenko AV, Andrievsky SM, Thorium lines in the spectra of several SMC supergiant stars, Odessa Astron. Publ. 20, 58-61 (2007). https://doi.org/10.18524/1810-4215.2007.20.87222

Gopka VF, Shavrina AV, Yushchenko VA, Vasil'eva SV, Yushchenko AV, et al., On the thorium absorption lines in the visible spectra of supergiant stars in the Magellanic Clouds, Bull. Crime. Astrophys. Obs. 109, 41-47 (2013). https://doi.org/10.3103/S0190271713010087

Gray DF, The Observation and Analysis of Stellar Photospheres (John Wiley & Sons Inc., Hoboken, 1976), 484.

Grevesse N, Asplund M, Sauval AJ, Scott P, The chemical composition of the Sun, Astrophys. Space Sci. 328, 179-183 (2010). https://doi.org/10.1007/s10509-010-0288-z

Grevesse N, Scott P, Asplund M, Sauval AJ, The elemental composition of the Sun. III. the heavy elements Cu to

Th, Astron. Astrophys. 573, A27 (2015). https://doi.org/10.1051/0004-6361/201424111

Ivans II, Simmerer J. Sneden C. Lawler JE, Cowan JJ, et al., Near-ultraviolet observations of HD 221170: new insights into the nature of r-process-rich stars, Astrophys. J. 645, 613-633 (2006). https://doi.org/10.1086/504069

Jeong Y, Yushchenko AV, Doikov DN, Gopka VF, Yushchenko VO, Chemical composition of RR Lyn - an eclipsing binary system with Am and λ Boo type components, J. Astron. Space Sci. 34, 75-82 (2017). https://doi.org/10.5140/JASS.2017.34.2.75

Kang YW, Yushchenko AV, Hong K, Guinan EF, Gopka VF, Signs of accretion in the abundance patterns of the components of the RS CVn-type eclipsing binary star LX Persei, Astron. J. 145, 167 (2013). https://doi.org/10.1088/0004-6256/145/6/167

Kim C, Yushchenko AV, Gopka VF, Dorokhova TN, Musaev FA, et al., Chemical composition and differential time-series CCD photometry of V2314 Ophiuchi: a new λ Bootis-type star, Astron. J. 134, 926-933 (2007). https://doi.org/10.1086/520643

Kochanek CS, Beacom JF, Kistler MD, Prieto JL, Stanek KZ, et al. A survey about nothing: monitoring a million supergiants for failed supernovae, Astrophys. J. 684, 1336-1342 (2008). https://doi.org/10.1086/590053

Kurucz RL, SYNTHE spectrum synthesis programs and line data [CD-ROM] (Smithsonian Astrophysical Observatory, Cambridge, 1993).

Landstreet JD, Abundances of the elements He to Ni in the atmosphere of Sirius A, Astron. Astrophys. 528, A132 (2011). https://doi.org/10.1051/0004-6361/201016259

McCray R, Fransson C, The remnant of supernova 1987A, Annu. Rev. Astron. Astrophys. 54, 19-52 (2016). https://doi.org/10.1146/annurev-astro-082615-105405

Nilsson H, Zhang ZG, Lundberg H, Johansson S, Nordstrőm B, Experimental oscillator strengths in Th II, Astron. Astrophys. 382, 368-377 (2002). https://doi.org/10.1051/0004-6361:20011597

Placco VM, Holmbeck EM, Frebel A, Beers TC, Surman RA, et al., RAVE J203843.2-002333: the first highly R-process-enhanced star identified in the RAVE Survey, Astrophys. J. 844, 18 (2017). https://doi.org/10.3847/1538-4357/aa78ef

Popov MV, Filina AA, Baranov AA, Chardonnet P, Chechetkin VM, Aspherical nucleosynthesis in a core-collapse supernova with 25 $M_{\odot}$ standard progenitor, Astrophys. J. 783, 43 (2014). https://doi.org/10.1088/0004-637X/783/1/43

Ren J, Christlieb N, Zhao G, The Hamburg/ESO R-process enhanced star survey (HERES). VII. thorium abundances in metal-poor stars, Astron. Astrophys. 537, A118 (2012). https://doi.org/10.1051/0004-6361/201118241

Romaniello M, Primas F, Mottini M, Pedicelli S, Lemasle B, et al., The influence of chemical composition on the properties of Cepheid stars. II. the iron content, Astron. Astrophys. 488, 731-747 (2008). https://doi.org/10.1051/0004-6361:20065661

Shulyak D, Ryabchikova T, Kildiyarova R, Kochukhov O, Realistic model atmosphere and revised abundances of the coolest Ap star HD 101065, Astron. Astrophys. 520, A88 (2010). https://doi.org/10.1051/0004-6361/200913750

Smartt SJ, Observational constraints on the progenitors of core-collapse supernovae: the case for missing high-mass stars, Publ. Astron. Soc. Aust. 32, e016 (2015). https://doi.org/10.1017/pasa.2015.17

Unterborn CT, Johnson JA, Panero WR, Thorium abundances in solar twins and analogs: implications for the habitability of extrasolar planetary systems, Astrophys. J. 806, A139 (2015). https://doi.org/10.1088/0004-637X/806/1/139

Yushchenko AV, URAN: a software system for the analysis of stellar spectra, Proceedings of the 20th Stellar Conference of the Czech and Slovak Astronomical Institutes. Brno, Czech Republic, 5-7 November 1997.

Yushchenko AV, Gopka VF, On thorium abundance in the atmosphere of Procyon, Astron. Lett. 20, 453-455 (1994).

Yushchenko AV, Gopka VF, Kim C, Liang YC, Musaev FA, et al., The chemical composition of the mild barium star HD 202109, Astron. Astrophys. 413, 1105-1114 (2004). https://doi.org/10.1051/0004-6361:20031596

Yushchenko A, Gopka V, Goriely S, Musaev F, Shavrina A, et al., Thorium-rich halo star HD 221170: further evidence against the universality of the r-process, Astron. Astrophys. 430, 255-262 (2005a). https://doi.org/10.1051/0004-6361:20041540

Yushchenko A, Gopka V, Kim C, Musaev F, Kang YW, et al., The chemical composition of δ Scuti, Mon. Not. R. Astron. Soc. 359, 865-873 (2005b). https://doi.org/10.1111/j.1365-2966.2005.08921.x

Yushchenko AV, Gopka VF, Kang YW, Kim C, Lee BC, et al., The chemical composition of ρ Puppis and the signs of accretion in the atmospheres of B-F-type stars, Astron. J. 149, 59 (2015). https://doi.org/10.1088/0004-6256/149/2/59

Yushchenko AV, Gopka VF, Shavrina AV, Yushchenko VA, Vasileva SV, et al., Peculiarities of the abundance of chemical elements in the atmosphere of PMMR23 - red supergiant in the Small Magellanic Cloud due to interstellar gas accretion, Kinemat. Phys. Celest. Bodies 33, 199-216 (2017a). https://doi.org/10.3103/S0884591317050075

Yushchenko AV, Jeong Y, Gopka VF, Vasil`eva SV, Andrievsky

SM, et al., Chemical composition of RM_1-390 - Large Magellanic Cloud red supergiant, J. Astron. Space Sci. 34, 199-205 (2017b). https://doi.org/10.5140/JASS.2017.34.3.199